Research Article

An Efficient Porcine Acoustic Signal Denoising Technique Based on EEMD-ICA-WTD

Sunan Zhang,[1] **Jianyan Tian** [ID],[1] **Amit Banerjee** [ID],[2] **and Jiangli Li**[1]

[1]*College of Electrical and Power Engineering, Taiyuan University of Technology, Taiyuan 030024, China*
[2]*School of Science, Engineering and Technology, Pennsylvania State University Harrisburg, Middletown 17057-4898, USA*

Correspondence should be addressed to Jianyan Tian; tut_tianjy@163.com

Automatic monitoring of group-housed pigs in real time through porcine acoustic signals has played a crucial role in automated farming. In the process of data collection and transmission, acoustic signals are generally interfered with noise. In this paper, an effective porcine acoustic signal denoising technique based on ensemble empirical mode decomposition (EEMD), independent component analysis (ICA), and wavelet threshold denoising (WTD) is proposed. Firstly, the porcine acoustic signal is decomposed into intrinsic mode functions (IMFs) by EEMD. In addition, permutation entropy (PE) is adopted to distinguish noise-dominant IMFs from the IMFs. Secondly, ICA is employed to extract the independent components (ICs) of the noise-dominant IMFs. The correlation coefficients of ICs and the first IMF are calculated to recognize noise ICs. The noise ICs will be removed. Then, WTD is applied to the other ICs. Finally, the porcine acoustic signal is reconstructed by the processed components. Experimental results show that the proposed method can effectively improve the denoising performance of porcine acoustic signal.

1. Introduction

With the development of precision livestock farming, it is hard for breeders to monitor porcine abnormal states. Sound recognition, as one of the noncontact detection methods, has been proven to be a valuable method to detect some diseases [1]. But during the process of acoustic signals collection and transmission, the recognition process is easy to be interfered by noise which will exert a negative impact on the recognition accuracy. Therefore, it is essential to eliminate the noise before analyzing the acoustic signals.

Empirical mode decomposition (EMD) is an effective automatic decomposition algorithm to analyze nonlinear, nonstationary, and non-Gaussian signals [2], and basis function is not required [3]. Because of this advantage, EMD is extensively applied in many different fields, such as blind source separation [4] and denoising [5]. The most common denoising method based on EMD is the threshold method of EMD, which determines the signal-dominated and noise-dominated intrinsic mode functions (IMFs) by the threshold. There are two types of denoising strategies for the threshold method of EMD. One is removing the noise-dominated IMFs directly [6], and the other is denoising IMFs by wavelet thresholding denoising (WTD) [7]. In order to distinguish the noise-dominated IMFs and signal-dominated IMFs, many methods have been proposed including the energy entropies of the IMFs [8], the correlation coefficients of the original signal and IMFs [9], and maximum variances of IMFs [10], among others. Ensemble empirical mode decomposition (EEMD) is proposed to overcome the problem of frequency aliasing of EMD [11]. Through adding Gaussian white noise, EEMD can avoid frequency aliasing to some extent. Some researchers have achieved good results in noise removal through replacing EMD with EEMD. Since the majority of useful information is lost when applying the first denoising strategy [12], some studies combine wavelet threshold denoising with the EMD threshold method [13]. However, the application of the wavelet threshold method in IMFs denoising may affect the continuity of reconstructed signals [14].

FIGURE 1: The installation drawing of the acoustic pickup in piggery.

In order to effectively eliminate the noise produced in the process of sound collection and transmission, EEMD-ICA-WTD, which can be employed before porcine sound recognition, is proposed in this paper. EEMD is used to decompose the porcine acoustic signal into IMFs. Then noise-dominant IMFs are distinguished by permutation entropy (PE). The independent components (IC) of noise-dominant IMFs are extracted by independent component analysis (ICA). As the first IMF contains much of the high-frequency noise [15], the correlation coefficients of ICs and the first IMF are calculated to recognize noise ICs. After that, the noise ICs are removed and the other ICs are denoised by WTD. Finally, the processed ICs are used to reconstruct the porcine acoustic signal. Experimental results show that the proposed method can eliminate the noise in porcine acoustic signal efficiently.

This paper is organized as follows: Section 1 introduces the background significance of porcine acoustic signal denoising and the methods commonly used to eliminate the noises of different signals in recent years. Section 2 describes the porcine acoustic signals and the individual methods, including EEMD, PE, Fast-ICA, and WTD. The process of the proposed EEMD-ICA-WTD is presented in Section 3. The denoising performance evaluation indices, the simulation process, results of EEMD-ICA-WTD, and comparisons with other methods are presented in Section 4. Conclusions are drawn in Section 5.

2. Materials and Methods

The materials of this study are porcine acoustic signals. Below are the details of porcine acoustic signals. The methods are mainly comprised of EEMD, PE, Fast-ICA, and WTD, with a detailed explanation given below.

2.1. Materials. In this study, the original data are collected by an acoustic pickup device (ELITE model OS-100) from a large-scale pig farm in Shanxi Province, China. The schematic of the installation of the acoustic pickup in the pig farm is shown in Figure 1. The replacement gilts (PIC) at 5~10 months old with weight ranging from 110 kg to 130 kg

were studied in these experiments. Five replacement gilts were housed in a pigpen which is four meters wide and six meters long. The collection of sounds is controlled by the program developed in the numerical computing software (Python, ver. Python 3.5). The sampling frequency of the collected acoustic data is 1 kHz. The porcine acoustic signals we selected are scream [16] and cough [17], which are found most commonly in the pigpen. See the data in the Supplementary Material (available here) for the denoising experiments of porcine acoustic signals. In order to analyze the performance of the proposed method qualitatively, Gaussian white noise is added to the porcine acoustic signals to obtain signals with different signal-to-noise ratios (SNRs). In this paper, SNRin is defined as an input SNR of the added white Gaussian noise value and SNRout is defined as an output SNR of denoised signal.

2.2. Methods. The process of EEMD-ICA-WTD is mainly comprised of porcine acoustic signal decomposition based on EEMD, noise-dominant IMFs differentiation based on PE, independent components extraction by Fast-ICA, and denoising by WTD.

2.2.1. Porcine Acoustic Signal Decomposition Based on EEMD. In this paper, the porcine acoustic signal is firstly decomposed. EMD can decompose the signals into IMFs from high to low frequency self-adaptively [18, 19], which is based on the decomposition principle that any signal is composed of IMFs [20]. The IMF must satisfy two conditions: (1) The number of extreme points is equal to the number of zero-crossings. Or the difference of the number of extreme points and the number of zero-crossings is at most 1; (2) At any point, the mean value of the envelope defined by the local maxima and the envelope defined by the local minima is zero. The process of EMD is as follows:

(1) The local extreme points which are detected from the original signal $s(t)$ can be connected by cubic curve spline and formed the upper and lower envelops.

And the list $m_1(t)$ is defined as the means of the upper and lower envelopes.

(2) The list $h_1(t)$ is defined as

$$h_1(t) = s(t) - m_1(t). \tag{1}$$

If $h_1(t)$ satisfies the above two conditions of IMF, it will be regarded as one of the IMF components:

$$c_1(t) = h_1(t), \tag{2}$$

where $c_1(t)$ is the first IMF.

(3) The residual list $r_1(t)$ is the difference between the original signal $s(t)$ and $c_1(t)$, which is defined as

$$r_1(t) = s(t) - c_1(t). \tag{3}$$

(4) The residual list $r_1(t)$ is regarded as original signal. And then, repeat the steps 1–3. Finally, the other IMFs $c_1(t), c_2(t), \ldots, c_n(t)$ and the final residual $r_n(t)$ (Res) can be obtained.

Therefore, the original signal $s(t)$ is decomposed as the sum of the IMF components and residual list $r_n(t)$:

$$s(t) = \sum_{i=1}^{n} c_i(t) + r_n(t), \tag{4}$$

where n is the number of IMF components.

Classical EMD may cause frequency aliasing during signal decomposition. In order to overcome this shortcoming, EEMD was proposed by Wu and Huang [11]. The structure of EEMD is similar to EMD. The EEMD decomposition is done according to the following steps [21]:

(1) Add a random Gaussian white noise signal $\hat{n}_i(t)$ to original signal $s(t)$, which is defined as

$$s_i(t) = s(t) + \hat{n}_i(t), \tag{5}$$

where $s_i(t)$ is a synthetic signal after the ith iteration adding white noise.

(2) Decompose $s_i(t)$ by EMD into several IMFs and a residual as

$$s_i(t) = \sum_{j=1}^{n} c_{ij}(t) + r_{in}(t), \tag{6}$$

where $c_{ij}(t)$ are the IMF components and $r_{in}(t)$ is the residual.

(3) Repeat the process as described above N times and add the different Gaussian white noises. Therefore, the original signal adds the Gaussian white noise N times. The means of IMFs can be obtained as

$$c_j(t) = \frac{1}{N} \sum_{i=1}^{N} c_{ij}, \tag{7}$$

where $c_j(t)$ is the jth IMF.

2.2.2. Identification of Noise-Dominant IMFs by PE. Permutation entropy (PE), proposed by Bandt and Pompe [22], is an average entropy parameter based on the statistical attributes of time series elements [23]. It is sensitive to the variations of signals. PE can be described as follows:

(1) For a given time series $X = \{x(i), i = 1, 2, \ldots, n\}$, the matrix of phase space reconstruction A is obtained as [24]

$$A = \begin{bmatrix} x(1) & x(1+\lambda) & \cdots & x(1+(m-1)\lambda) \\ x(2) & x(2+\lambda) & \cdots & x(2+(m-1)\lambda) \\ \cdots & \cdots & \cdots & \cdots \\ x(r) & x(r+\lambda) & \cdots & x(r+(m-1)\lambda) \end{bmatrix}, \tag{8}$$

where λ is the time delay, m denotes the embedding dimension, and r is the number of vectors in phase space reconstruction components, $r = n - (m-1)\lambda$.

(2) Each row of A can be arranged in ascending order [25]:

$$x(i + (j_1 - 1)\lambda) \le x(i + (j_2 - 1)\lambda)$$
$$\le \cdots \le x(i + (j_m - 1)\lambda), \tag{9}$$

where $j_1, j_2, \ldots, j_m$ are the column indexes of elements in reconstruction components.

(3) Since the embedding dimension is m, there will be $m!$ possible permutations. Each row of A can be represented by one of the permutations. P_j represents the probability of jth permutation. Then, the PE can be designated as follows [26]:

$$H_p(m) = -\sum_{j=1}^{k} P_j \ln P_j, \tag{10}$$

where P_j is the probability of jth permutation and k is the number of possible permutations, $k = m!$.

(4) The PE of order can be normalized as [26]

$$H_p = \frac{H_p(m)}{\ln(m!)}. \tag{11}$$

The range of PE is 0 to 1. The PE can be used to recognize the IMF of noise [27]. Therefore, PE is adopted to distinguish noise-dominant IMFs in this paper.

2.2.3. Independent Components Extraction by Fast-ICA. The ICA, as one of the multivariate statistical methods, is widely used in statistical sources separation [28]. It can extract the independent components from the mixture with unknown mixing coefficients [3].

The independent sources can be denoted as $s(t) = [s_1(t), s_2(t), \ldots, s_K(t)]^{\mathrm{T}}$, where K is the number of independent sources. The observed signals can be defined as $x(t) = [x_1(t), x_2(t), \ldots, x_M(t)]^{\mathrm{T}}$, where M is the number of observed
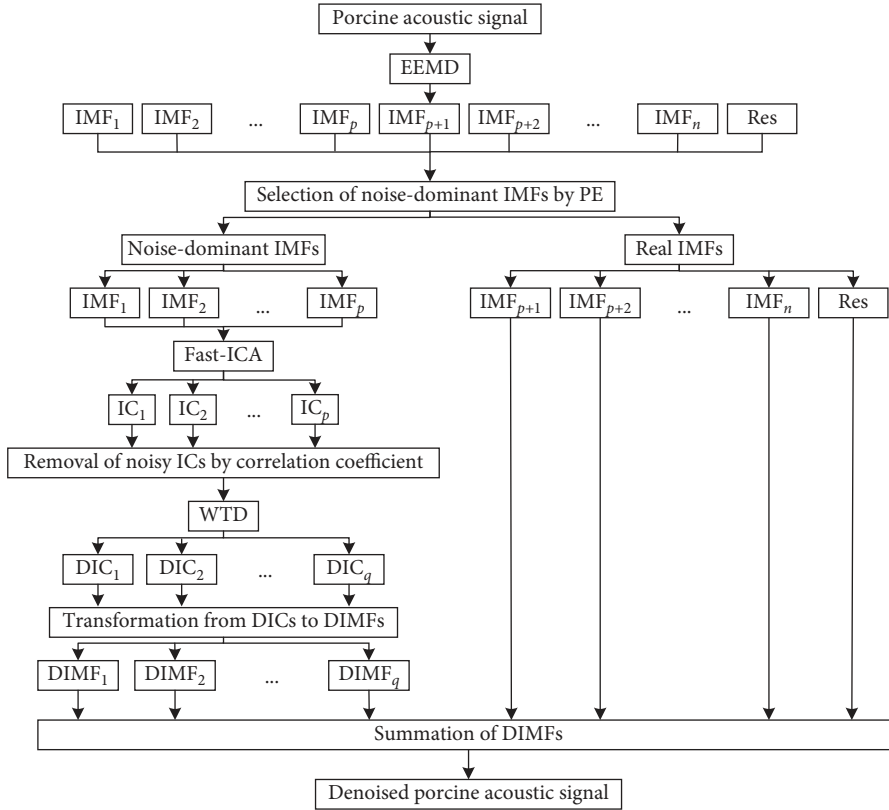
FIGURE 2: The process chart of the proposed denoising technique for porcine acoustic signal.

signals. $A = \begin{bmatrix} a_{11} & \cdots & a_{1j} \\ M & \cdots & M \\ a_{i1} & \cdots & a_{ij} \end{bmatrix}$ represents the matrix of mixing coefficients. The mixing relationship is defined as follows:

$$x_i(t) = \sum_{j=1}^{K} a_{ij} s_j(t), \quad i = 1, 2, \ldots, M. \tag{12}$$

This function can be expressed by the matrix:

$$x(t) = A \cdot s(t). \tag{13}$$

The aim of ICA is to estimate the inverse of the mixing matrix W, which could be used to calculate the independent signals.

$$y(t) = W \cdot x(t) = W \cdot A \cdot s(t), \tag{14}$$

where $y(t)$ is the estimation of $s(t)$, $y(t) = [y_1(t), y_2(t), \ldots, y_N(t)]^T$.

Fast-ICA algorithm is one of the improved ICA algorithms, which is widely utilized to estimate the orthogonal matrix. Fast-ICA has higher convergence speed compared to the conventional method and the step-size parameters are not needed. In this paper, Fast-ICA is used to extract independent components from IMFs.

2.2.4. *Denoising by WTD.* Wavelet transform denoising (WTD) is one of the denoising algorithms based on wavelet

transform (WT). WT can decompose signals at different scales. The discrete wavelet transform (DWT) is calculated as follows:

$$WT(a,b) = \frac{1}{\sqrt{2^a}} \sum_{t=1}^{T} s(t) \times \psi\left(\frac{t - b \cdot 2^a}{2^a}\right), \tag{15}$$

where a is the decomposition level, b is the parameter of translation (for dyadic WT: $b = 1$), ψ is the wavelet basis function, and T is the number of sampling points.

The primary steps of WTD are described as follows:

(1) Decompose the original signal by WT with proper wavelet basis function and decomposition level.

(2) The threshold is performed by the selected proper threshold method for high-frequency coefficients at each decomposition scale. The low-frequency wavelet coefficient is kept unchanged.

(3) The signal is reconstructed by the low-frequency coefficients and high-frequency coefficients after threshold processing.

It is crucial to select an appropriate threshold method for WTD. The common threshold selection methods fall into soft threshold method and hard threshold method [29]. The hard threshold method causes breakpoint at the threshold point. The reconstruction coefficient of the soft threshold method has good continuity [30]. Therefore, the soft threshold method is adopted in this paper.
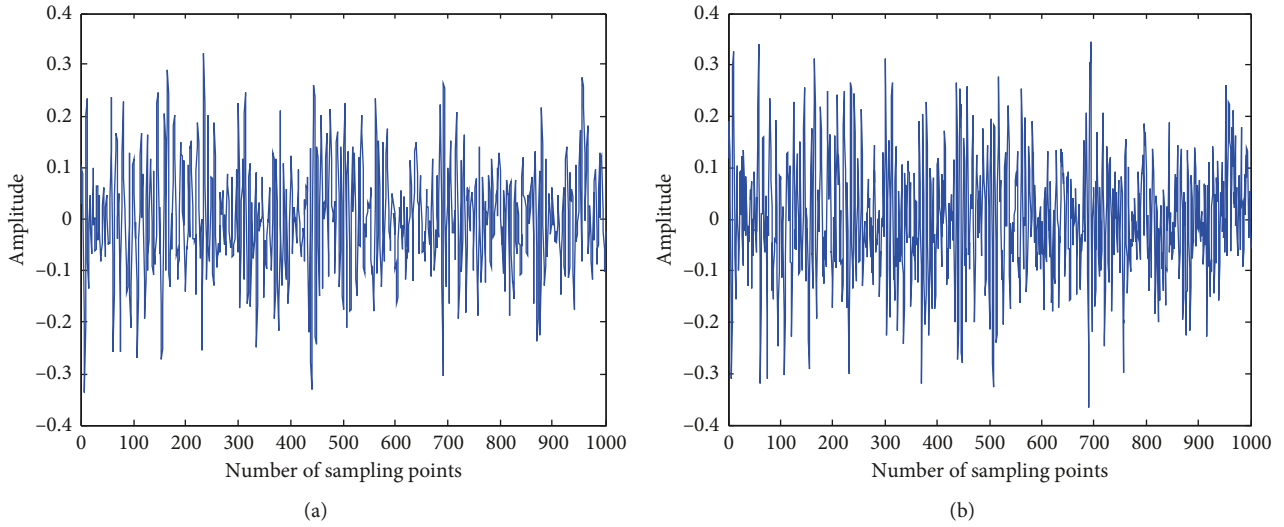
(a)

(b)

FIGURE 3: The time-domain waveforms of (a) porcine scream and (b) noisy scream.
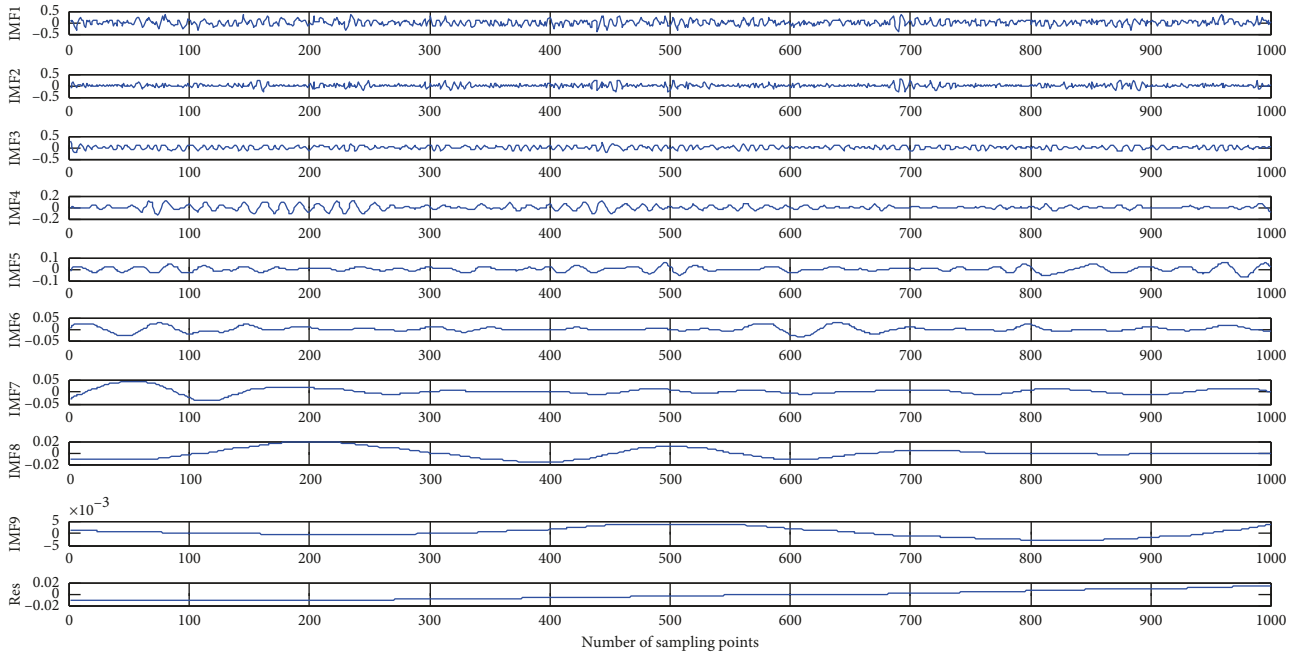

FIGURE 4: The decomposition result of the noisy scream.

3. Proposed Methodology

The process of the new efficient denoising technique proposed in this paper is shown in Figure 2. It consists of five main steps explained as follows:

(1) The porcine acoustic signal is decomposed into IMFs by EEMD. Sorted in the increasing order of IMFs, the frequency distribution of the IMFs varies from high to low. The noise mainly concentrates in high frequency. Therefore, the first few IMFs contain both the information of porcine acoustic signal and noise [15]. PE of each IMF is calculated. If PE is more than 0.5, the corresponding IMF will be regarded as noise-dominant one.

(2) Denoising the noise-dominant IMFs directly may destroy the continuity of reconstructed signals. It is harmful to the denoising effect [14]. Therefore, Fast-ICA is used to extract the ICs of noise-dominant IMFs to concentrate the noise and real information and improve SNR of components.

(3) As the first IMF contains much of the high-frequency noise [15], the correlation coefficients of ICs and the first IMF are calculated. If the correlation coefficient is more than 0.8, the IC will be regarded as noise and will be removed.

(4) Denoise the other ICs by WTD. The wavelet basis function and decomposition level we selected are db6 and 3.

TABLE 1: PEs of noisy scream IMFs.

IMF1	IMF2	IMF3	IMF4	IMF5	IMF6	IMF7	IMF8	IMF9	Res
0.974	0.997	0.824	0.674	0.567	0.493	0.440	0.415	0.396	0

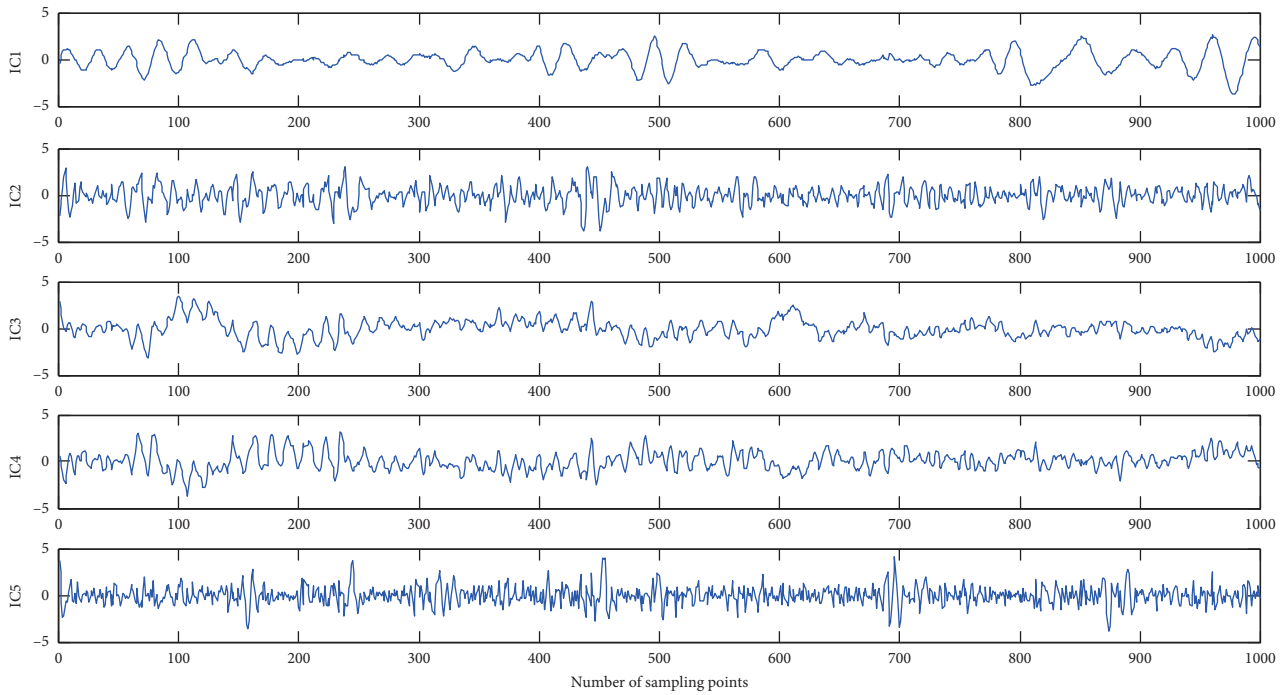FIGURE 5: The time-domain waveforms of ICs.

TABLE 2: Correlation coefficients of each IC and the first IMF.

IC1	IC2	IC3	IC4	IC5
0.3222	0.4656	0.2772	0.8460	0.3170

(5) The denoised ICs (DICs) are transformed to denoised IMFs (DIMFs) through the matrix of mixing coefficients. Then the porcine acoustic signal is reconstructed by these DIMFs and real IMFs.

4. Results and Discussion

This section introduces the simulation process and results of EEMD-ICA-WTD. In order to verify the performance of EEMD-ICA-WTD, the performance of the denoising is compared with the other six methods.

4.1. Simulation Process and Result of EEMD-ICA-WTD. In order to analysis the process and results of EEMD-ICA-WTD, porcine scream and porcine cough are selected for denoising, taking the noisy scream with 5 dB SNRin by adding Gaussian white noise as an example. The time-domain waveforms of porcine scream and noisy scream are shown in Figure 3. The sampling frequency of the collected acoustic data is 1 kHz. Therefore, the porcine scream of 1 s contains 1000 sampling points.

The noisy scream is decomposed as step 1. The time-domain waveforms of IMFs and Res are shown in Figure 4. The noisy scream is divided into 9 IMFs

of different frequencies and 1 residual. Each IMF contains different local characteristics of the original noisy scream.

The PE of each IMF is calculated as step 1. The time delay λ is commonly used as 1 and the embedding dimension m is commonly used as 3 [31]. In this paper, $\lambda = 1$, $m = 3$. The PE of each IMF is shown in Table 1.

Table 1 shows that the PEs of IMF1, IMF2, IMF3, IMF4, and IMF5 are greater than 0.5. Therefore, these are noise-dominant IMFs.

The ICs of noise-dominant IMFs are extracted by Fast-ICA as step 2. The time-domain waveforms of ICs are shown in Figure 5. It can be observed that each IC concentrates more information.

The correlation coefficients are calculated as step 3. The correlation coefficients of ICs and the first IMF are shown in Table 2.

Table 2 shows that the correlation coefficient between IC4 and the first IMF is larger than 0.8. Therefore, it should be removed.

The other ICs are denoised by WTD as step 4. The denoising results are shown in Figure 6.

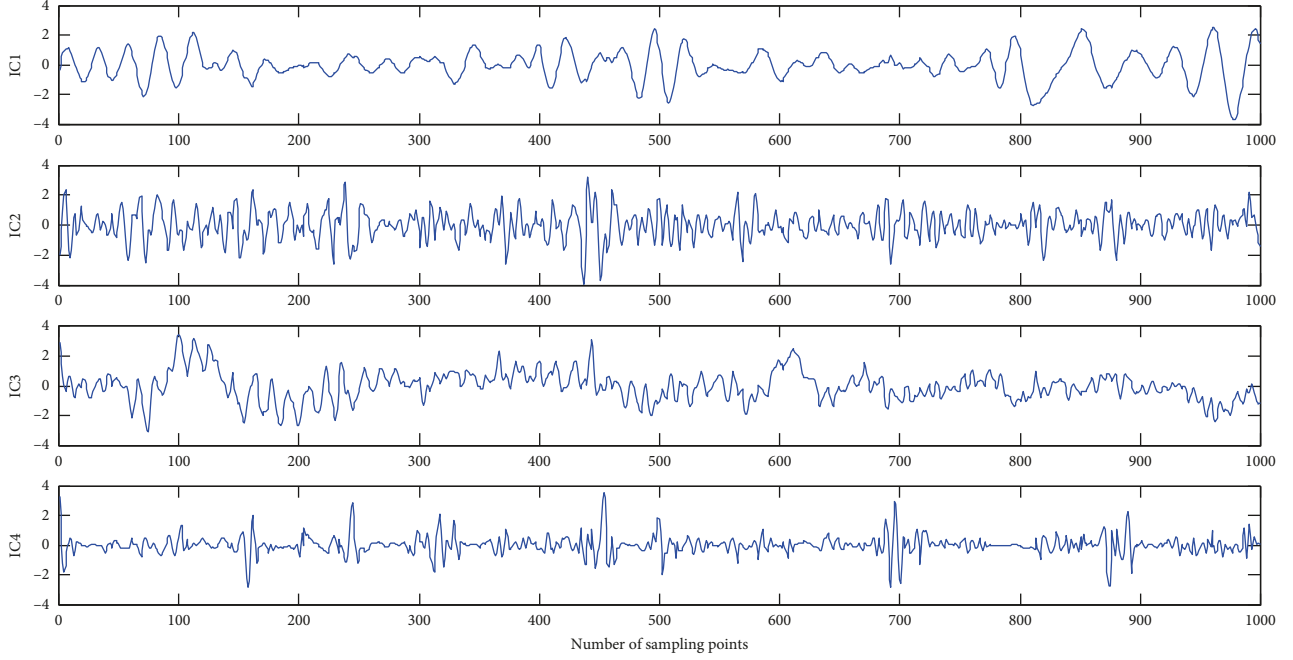The end result of the reconstructed signal is shown in Figure 7.
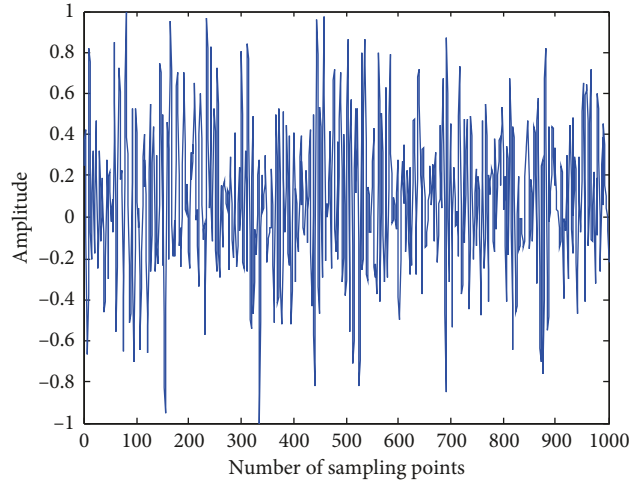
FIGURE 6: The denoising results of ICs by WTD.

FIGURE 7: The time-domain waveforms of the reconstructed porcine scream.

In order to evaluate the denoising performance of the method quantitatively, the root mean square error (RMSE), SNRout, and correlation coefficient (R) are adopted in this article [32]:

$$\text{RMSE} = \sqrt{\frac{1}{T} \sum_{t=1}^{T} \left[s(t) - s'(t) \right]^2},$$

$$\text{SNR} = 10 \lg \left(\frac{\sum_{t=1}^{T} s^2(t)}{\sum_{t=1}^{T} \left(s(t) - s'(t) \right)^2} \right), \quad (16)$$

$$R = \frac{\text{cov}(s', s)}{\sigma'_s \cdot \sigma_s},$$

TABLE 3: The denoising parameters of porcine scream.

RMSE	SNRout	R
0.1476	6.2831	0.8992

where $s(t)$ is the porcine acoustic signal, $s'(t)$ is the denoised porcine acoustic signal, T is the number of sampling points, $\text{cov}(s', s)$ is the covariance of s' and s, $\sigma_{s'}$ is the standard deviation of s', and σ_s is the standard deviation of s.

RMSE reflects the degree of error between the denoised porcine acoustic signal and the original porcine acoustic signal. The smaller the value, the better the denoising effect. SNRout reflects the ratio of the porcine acoustic signal to real noise. Therefore, the higher the value, the less noise mixes. R

TABLE 4: Denoising results of porcine scream.

SNRin	Parameter	Denoising methods						
		EMD-TD	EMD-WTD	EEMD-TD	EEMD-WTD	WSTD	MBSS	EEMD-ICA-WTD
−10	RMSE	0.4794	0.3594	0.3952	0.3682	0.4319	0.7362	0.3389
	SNRout/dB	−3.9501	−1.4474	−2.2729	−1.6579	−3.0440	−8.6582	−1.0408
	R	0.0633	0.3585	0.1723	0.3303	0.1762	0.0324	0.3701
−5	RMSE	0.4379	0.3597	0.3774	0.3643	0.4101	0.5214	0.3339
	SNRout/dB	−3.1633	−1.2094	−1.8728	−1.5668	−2.5937	−3.9452	−0.8091
	R	0.1449	0.5380	0.2498	0.5343	0.3897	0.1167	0.5544
0	RMSE	0.4497	0.2533	0.3389	0.2601	0.2867	0.3241	0.2496
	SNRout/dB	−3.3946	1.5894	−0.9377	1.3619	0.5148	−0.8852	1.4573
	R	0.1972	0.7590	0.4029	0.7779	0.7683	0.7091	0.7810
5	RMSE	0.4460	0.1474	0.3483	0.1491	0.1506	0.1543	0.1432
	SNRout/dB	−3.3242	6.2958	−1.1767	6.1937	6.1054	6.2438	6.4831
	R	0.2381	0.9047	0.3955	0.9064	0.9029	0.8823	0.9145
10	RMSE	0.4315	0.0971	0.3321	0.0944	0.0935	0.0951	0.0913
	SNRout/dB	−3.0361	9.9147	−0.7613	10.1594	10.2463	10.0864	10.3106
	R	0.2038	0.9480	0.4088	0.9518	0.9531	0.9487	0.9569

TABLE 5: Denoising results of porcine cough.

SNRin	Parameter	Denoising methods						
		EMD-TD	EMD-WTD	EEMD-TD	EEMD-WTD	WSTD	MBSS	EEMD-ICA-WTD
−10	RMSE	0.4216	0.3100	0.3245	0.3163	0.3417	0.4775	0.3025
	SNRout/dB	−2.4745	0.1955	−0.1995	0.0217	−0.6479	−2.9245	0.2213
	R	0.2337	0.4732	0.4832	0.4951	0.4389	0.2183	0.4978
−5	RMSE	0.3447	0.2629	0.2666	0.2773	0.2946	0.3341	0.2442
	SNRout/dB	−0.7254	1.6290	1.5076	1.1645	0.6390	−0.4762	1.9498
	R	0.3903	0.6406	0.6656	0.6736	0.6075	0.4097	0.6752
0	RMSE	0.4168	0.2048	0.2464	0.2042	0.2423	0.2658	0.1880
	SNRout/dB	−2.3755	3.7967	0.1914	3.8236	2.3360	2.1935	4.0920
	R	0.2767	0.7936	0.7359	0.8310	0.8257	0.7016	0.8353
5	RMSE	0.3941	0.1298	0.2762	0.1343	0.1362	0.1407	0.1224
	SNRout/dB	−1.8887	7.7609	1.1993	7.4601	7.3379	7.2837	7.9737
	R	0.2712	0.9237	0.7403	0.9332	0.9293	0.8819	0.9360
10	RMSE	0.2777	0.0721	0.0952	0.0692	0.0842	0.0743	0.0646
	SNRout/dB	2.1711	13.8798	11.4739	14.2417	12.5417	13.7961	14.6788
	R	0.6897	0.9805	0.9689	0.9854	0.9828	0.9829	0.9859

is used to evaluate the correlation between the denoised porcine acoustic signal and the original porcine acoustic signal. The higher value represents the better denoising effect.

The performance of the denoising is shown in Table 3.

4.2. Comparison with Other Methods.

In order to verify the performance of EEMD-ICA-WTD, six different denoising methods are used as comparison methods. They are EMD-TD [33], EMD-WTD [34], EEMD-TD [35], EEMD-WTD [36], wavelet soft threshold denoising (WSTD) [37], and multiband spectral subtraction (MBSS) [38]. To verify the universality of the methods, two kinds of porcine acoustic signals with different SNRins are denoised. The denoising results of different methods are shown in Tables 4 and 5, where Table 4 is the denoising results of porcine scream and Table 5 is the denoising results of porcine cough.

The results, shown in Tables 4 and 5, are compared with different denoising methods evaluated using three parameters. According to the evaluations of RMSE, SNRout, and R, the EEMD-ICA-WTD has lower RMSE, higher SNRout, and R than the other six methods.

The results show that the EEMD-ICA-WTD proposed in this paper has the best denoising effects with different SNRins not only for porcine scream but also for porcine cough. The EEMD-WTD has the second-best denoising effects. Taking the denoising results for porcine cough as an example, when the SNRin of porcine cough is 10 dB, the values of RMSE, SNRout, and R after being denoised by EEMD-ICA-WTD are 0.0646, 14.6788, and 0.9859, respectively. These are close to the results of EEMD-WTD. The absolute differences of these three parameters between
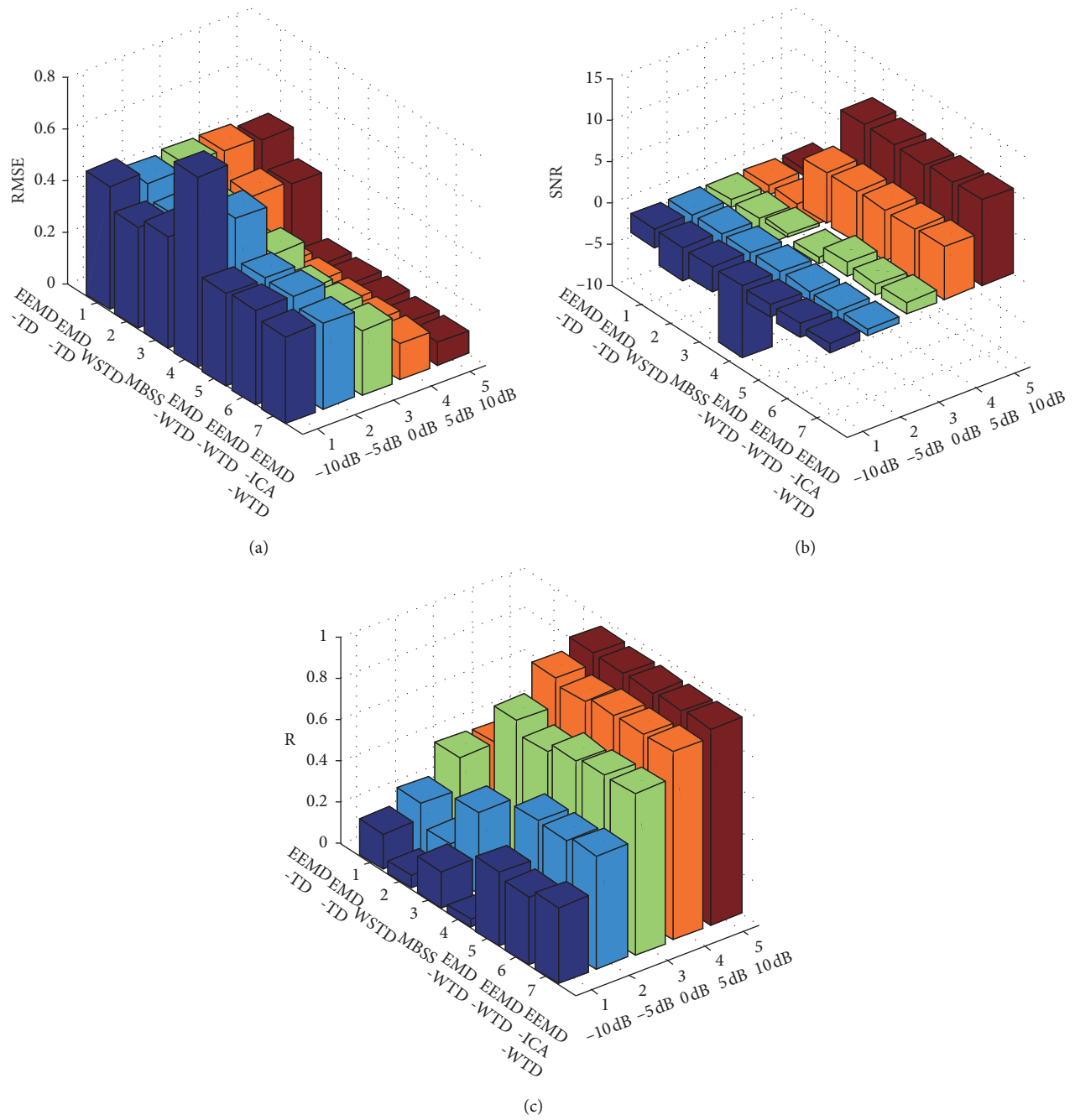
(a)

(b)

(c)

Figure 8: Denoising results for porcine scream with different SNRins: (a) RMSE, (b) SNRout, and (c) R.

EEMD-ICA-WTD and EEMD-WTD are 0.0046, 0.4371, and 0.0005, respectively. With the increasing noise, the advantages of EEMD-ICA-WTD are more obvious. When the SNRin of porcine cough is −10 dB, the absolute differences of RMSE, SNRout, and R between EEMD-ICA-WTD and EEMD-WTD are 0.0138, 0.1996, and 0.0027, respectively. A large number of experiments for different kinds of porcine acoustic signals verify the universality of EEMD-ICA-WTD. In order to intuitively compare the performances of different denoising methods for porcine

scream and porcine cough with different SNRins, the histograms are shown in Figures 8 and 9. Each histogram contains the denoising results of different methods with different SNRins. Different colors represent different SNRins. It can be observed that the RMSEs of EEMD-ICA-WTD with different SNRins are lower than the other six methods. And the SNRouts and Rs of EEMD-ICA-WTD are higher than the other six methods. In summary, the results show that the EEMD-ICA-WTD method is effective and suitable for porcine acoustic signal.
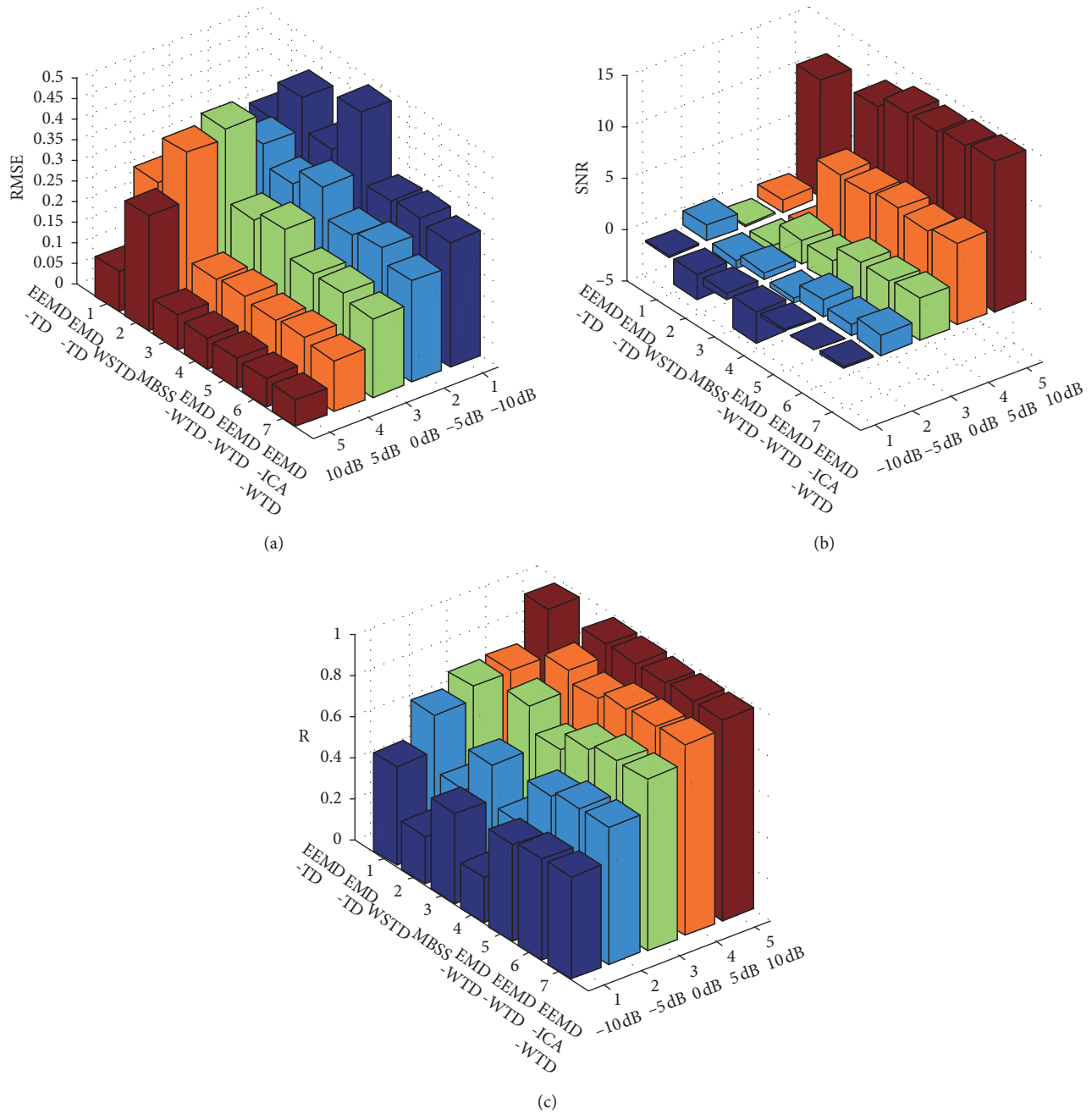
(a)

(b)

(c)

Figure 9: Denoising results for porcine cough with different SNRins: (a) RMSE, (b) SNRout, and (c) R.

5. Conclusions

To improve the denoising performance of porcine acoustic signal, an efficient denoising technique based on EEMD-ICA-WTD is proposed in this paper. The approach has been developed with the purpose to reduce noise interference during the recognition of porcine abnormal sounds.

Firstly, the porcine acoustic signal is decomposed into different components in order of frequency. Because of the frequency aliasing of EMD, the EEMD is used to decompose the porcine acoustic signal into IMFs. As the noise mainly concentrates in high frequency, PE is used to distinguish the

noise-dominant IMFs from the IMFs. Secondly, the continuity of the signal may be adversely affected if the noise-dominant IMFs are denoised directly. Therefore, the ICs of noise-dominant IMFs are extracted by Fast-ICA. The noise and real information are concentrated on the ICs. It has been shown that the first IMF contains much high-frequency noise. Therefore, the noise ICs are identified by correlation coefficients of ICs and the first IMF and are then removed. Finally, WTD is used for denoising the other ICs. The porcine acoustic signal is then reconstructed by processed ICs. The performance of this denoising method is shown to be superior to other methods.

In the future work, this approach will be optimized to reduce the run time on the premise of guaranteeing the performance of the denoising.

Data Availability

The porcine acoustic data used to support the findings of this study are included within the supplementary information file.

Conflicts of Interest

The authors declare that there are no conflicts of interest regarding the publication of this paper.

Acknowledgments

Supplementary Materials

The supplementary materials are porcine acoustic signals of scream and cough. The data are saved as WAV format. The length of each signal is 1 s. (*Supplementary Materials*)

References

[1] J. Lee, L. Jin, D. Park et al., "Acoustic features for pig wasting disease detection," *Internal Journal of Information Processing and Management*, vol. 6, no. 1, pp. 37–46, 2015.

[2] R. Abdelkader, A. Kaddour, and Z. Derouiche, "Enhancement of rolling bearing fault diagnosis based on improvement of empirical mode decomposition denoising method," *The International Journal of Advanced Manufacturing Technology*, vol. 97, no. 5–8, pp. 3099–3117, 2018.

[3] S. Sengottuvel, P. F. Khan, N. Mariyappa, R. Patel, S. Saipriya, and K. Gireesan, "A combined methodology to eliminate artifacts in multichannel electrogastrogram based on independent component analysis and ensemble empirical mode decomposition," *SLAS Technology: Translating Life Sciences Innovation*, vol. 23, no. 3, pp. 269–280, 2018.

[4] M. Kemiha and A. Kacha, "Complex blind source separation," *Circuits, Systems, and Signal Processing*, vol. 36, no. 11, pp. 4670–4687, 2017.

[5] S. Jain, V. Bajaj, and A. Kumar, "Riemann liouvelle fractional integral based empirical mode decomposition for ECG denoising," *IEEE Journal of Biomedical and Health Informatics*, vol. 22, no. 4, pp. 1133–1139, 2018.

[6] Q. Mao, X. Fang, Y. Hu, and G. Li, "Chiller sensor fault detection based on empirical mode decomposition threshold denoising and principal component analysis," *Applied Thermal Engineering*, vol. 144, pp. 21–30, 2018.

[7] J. X. Zeng, G. F. Wang, F. Q. Zhang, and J. C. Ye, "The denoising algorithm based on intrinsic time-scale decomposition," *Advanced Materials Research*, vol. 422, pp. 347–352, 2011.

[8] Y. Yu, D. Yu, and C. Junsheng, "A roller bearing fault diagnosis method based on EMD energy entropy and ANN," *Journal of Sound and Vibration*, vol. 294, no. 1-2, pp. 269–277, 2006.

[9] A. Ayenu-Prah and N. Attoh-Okine, "A criterion for selecting relevant intrinsic mode functions in empirical mode decomposition," *Advances in Adaptive Data Analysis*, vol. 2, no. 1, pp. 1–24, 2010.

[10] Q. Zhang and H. Y. Xing, "Adaptive denoising algorithm based on the variance characteristics of EMD," *Acta Electronica Sinica*, vol. 43, no. 5, pp. 901–906, 2015.

[11] Z. Wu and N. E. Huang, "Ensemble empirical mode decomposition: a noise-assisted data analysis method," *Advances in Adaptive Data Analysis*, vol. 1, no. 1, pp. 1–41, 2009.

[12] R. Wang, S. Sun, X. Guo, and D. Yan, "EMD threshold denoising algorithm based on variance estimation," *Circuits, Systems, and Signal Processing*, vol. 37, no. 12, pp. 5369–5388, 2018.

[13] Y. M. Ni and N. H. Yang, "Speech denoising application based on Hilbert-Huang transform," *Computer simulation*, vol. 28, no. 4, pp. 408–412, 2011.

[14] Y. Kopsinis and S. Mclaughlin, "Development of EMD-based denoising methods inspired by wavelet thresholding," *IEEE Transactions on Signal Processing*, vol. 57, no. 4, pp. 1351–1362, 2009.

[15] P. Singh, S. Shahnawazuddin, and G. Pradhan, "An efficient ECG denoising technique based on non-local means estimation and modified empirical mode decomposition," *Circuits, Systems, and Signal Processing*, vol. 37, no. 10, pp. 4527–4547, 2018.

[16] J. Vandermeulen, C. Bahr, E. Tullo et al., "Discerning pig screams in production environments," *PLoS One*, vol. 10, no. 4, Article ID e0123111, 2015.

[17] M. Silva, V. Exadaktylos, S. Ferrari, M. Guarino, J.-M. Aerts, and D. Berckmans, "The influence of respiratory disease on the energy envelope dynamics of pig cough sounds," *Computers and Electronics in Agriculture*, vol. 69, no. 1, pp. 80–85, 2009.

[18] Y. Yu, W. Li, D. Sheng, and J. Chen, "A novel sensor fault diagnosis method based on modified ensemble empirical mode decomposition and probabilistic neural network," *Measurement*, vol. 68, pp. 328–336, 2015.

[19] N. Zhao and R. Li, "EMD method applied to identification of logging sequence strata," *Acta Geophysica*, vol. 63, no. 5, pp. 1256–1275, 2015.

[20] B. Wang, L. Wang, X. Tang, and S. Yang, "A braking intention identification method based on data mining for electric vehicles," *Mathematical Problems in Engineering*, vol. 2019, Article ID 7543496, 8 pages, 2019.

[21] S. Dun, J. Fu, F. Zhu, and N. Xiong, "A compound structure for wind speed forecasting using MKLSSVM with feature selection and parameter optimization," *Mathematical Problems in Engineering*, vol. 2018, Article ID 9287097, 21 pages, 2018.

[22] C. Bandt and B. Pompe, "Permutation entropy: a natural complexity measure for time series," *Physical Review Letters*, vol. 88, no. 17, article 174102, 2002.

[23] C. Li, L. Zhan, and L. Shen, "Friction signal denoising using complete ensemble EMD with adaptive noise and mutual information," *Entropy*, vol. 17, no. 12, pp. 5965–5979, 2015.

[24] J. Zheng, Z. Dong, H. Pan, Q. Ni, T. Liu, and J. Zhang, "Composite multi-scale weighted permutation entropy and extreme learning machine based intelligent fault diagnosis for rolling bearing," *Measurement*, vol. 143, pp. 69–80, 2019.

[25] Y. Gu, Z. Liang, and S. Hagihira, "Use of multiple EEG features and artificial neural network to monitor the depth of anesthesia," *Sensors*, vol. 19, no. 11, p. 2499, 2019.

[26] X. Zheng, G. Zhou, D. Li, and H. Ren, "Application of variational mode decomposition and permutation entropy for rolling bearing fault diagnosis," *2019*, vol. 24, no. 2, pp. 303–311, 2019.

[27] B. Lili, H. Zhennan, L. Yanfeng, and N. Shaohui, "A hybrid denoising algorithm for the gear transmission system based on CEEMDAN-PE-TFPF," *Entropy*, vol. 20, no. 5, p. 361, 2018.

[28] A. Hyvärinen and E. Oja, "Independent component analysis: algorithms and applications," *Neural Networks*, vol. 13, no. 4-5, pp. 411–430, 2000.

[29] D. L. Donoho, "De-noising by soft-thresholding," *IEEE Transactions on Information Theory*, vol. 41, no. 3, pp. 613–627, 1995.

[30] G. Wang, L. Chen, S. Guo, Y. Peng, and K. Guo, "Application of a new wavelet threshold method in unconventional oil and gas reservoir seismic data denoising," *Mathematical Problems in Engineering*, vol. 2015, Article ID 969702, 7 pages, 2015.

[31] M. El Sayed Hussein Jomaa, P. Van Bogaert, N. Jrad et al., "Multivariate improved weighted multiscale permutation entropy and its application on EEG data," *Biomedical Signal Processing and Control*, vol. 52, pp. 420–428, 2019.

[32] J. Zhang, Y. Guo, Y. Shen, D. Zhao, and M. Li, "Improved CEEMDAN-wavelet transform de-noising method and its application in well logging noise reduction," *Journal of Geophysics and Engineering*, vol. 15, no. 3, pp. 775–787, 2018.

[33] K. Khaldi, A.-O. Boudraa, A. Bouchikhi, and M. T.-H Alouane, "Speech enhancement via EMD," *EURASIP Journal on Advances in Signal Processing*, vol. 2008, no. 1, article 873204, p. 8, 2018.

[34] H. Sun, W. Chen, and J. Gong, "An improved empirical mode decomposition-wavelet algorithm for phonocardiogram signal denoising and its application in the frist and second heart sound extraction," in *Proceedings of the 2013 6th International Conference on Biomedical Engineering and Informatics (BMEI)*, pp. 187–191, Hangzhou, China, December 2013.

[35] M. J. Zhang, H. Chen, C. Wang, and Q. Cao, "Threshold noise reduction research of improved EEMD method," *Applied Mechanics and Materials*, vol. 226–228, pp. 237–240, 2012.

[36] W. Wang, Q. Chen, D. Yan, and D. Geng, "A novel comprehensive evaluation method of the draft tube pressure pulsation of Francis turbine based on EEMD and information entropy," *Mechanical Systems and Signal Processing*, vol. 116, pp. 772–786, 2019.

[37] J.-J. Jiang, L.-R. Bu, X.-Q. Wang et al., "Clicks classification of sperm whale and long-finned pilot whale based on continuous wavelet transform and artificial neural network," *Applied Acoustics*, vol. 141, pp. 26–34, 2018.

[38] T. Biswas, S. B. Mandal, D. Saha, and A. Chakrabarti, "FPGA based dual microphone speech enhancement," *Microsystem Technologies*, vol. 25, no. 3, pp. 765–775, 2019.